ELSEVIER

Journal of Nuclear Materials 258–263 (1998) 729–734

journal of nuclear materials

# Dynamical simulation for sputtering of $B_4C$

T. Kenmotsu [a,*], T. Kawamura [b], T. Ono [c], Y. Yamamura [c]

[a] *The Graduate University for Advanced Studies, National Institute for Fusion Science, Data and Planning Center, 332-6 Oroshi-cho, Toki-shi 509-5292, Japan*

[b] *National Institute for Fusion Science, 332-6 Oroshi-cho, Toki-shi 509-5292, Japan*

[c] *Okayama University of Science, 1-1, Ridai-cho, Okayama 700-0005, Japan*

**Abstract**

Using ACAT-DIFFUSE code, we have simulated the fluence dependence of $B_4C$ sputtering and the associated surface composition change under $D^+$ ion bombardment. The ACAT-DIFFUSE is a simulation code, which is based on a Monte Carlo method with a binary collision approximation and solves diffusion equations. In the case of near-threshold sputtering, the preferential sputtering of B atoms is enhanced by the threshold effect. As a result, the total sputtering yield at the steady state is reduced by about 20% compared with low-fluence sputtering. The surface concentration at steady state is determined by the competitive processes between diffusion and surface-atom removal due to sputtering. At normal incidence the interstitial diffusion contributes appreciably to the steady-state surface concentration, but at grazing incidence this effect is small. Therefore, the steady-state surface concentration ratio at grazing incidence is less than that of normal incidence. 

## 1. Introduction

Plasma-facing components, such as limiters and divertors, receive large fluxes of high energy particles. As a result, the constituent atoms of those materials are sputtered from the surface into the core plasma as impurities. Impurities cause core plasma cooling.

To reduce impurity generation, both low $Z$ and high $Z$ materials are adopted as candidates for plasma-facing components. High flux beam bombardment of $B_4C$ was studied at high temperature [1–3]. Those experiments show that the sputtering yield of $B_4C$ (boron carbide) are suppressed compared to that of graphite. This property could give the $B_4C$ material some advantage in the plasma-facing component.

The main concern of this paper is to simulate the fluence dependence of $B_4C$ sputtering and the associated surface composition changes under $D^+$ ion bombardment at normal and grazing incidences. For this purpose we have applied the ACAT-DIFFUSE [4,5] to light ion sputtering from $B_4C$.

## 2. Simulation model

A detailed description of the ACAT-DIFFUSE code has been given elsewhere [4,5]. Only a very brief outline is given here. The code assumes an amorphous target material and it is based on the binary collision approximation. In the code, the total dose $\Phi$ is divided into small dose increments $\Delta\Phi$ during which the bombarding ions do not change the target composition appreciably. The ions corresponding to $\Delta\Phi$ are assumed to hit the target material simultaneously and be slowed down instantaneously. Their slowing down, together with the associated vacancy and range distributions are simulated by the ACAT routine. These collided atoms diffuse during the time interval of $\Delta\Phi/J$ ($J$ being the current density). The diffusion process is estimated by solving the diffusion equations numerically in the DIFFUSE routine. In the code, these procedures are repeated $n$ times, where $n = \Phi/\Delta\Phi$. The logical representation of the code is ACAT-DIFFUSE = $[(\text{ACAT})(\text{DIFFUSE})]^n$.

## 3. Numerical results and discussions

One of the most important parameters for divertor erosion is the threshold sputtering due to light ions at

* Corresponding author. Tel.: +81 572 58 2222; fax: +81 572 58 2628; e-mail: kenmotsu@nifs.ac.jp.

0022-3115/98/$19.00 
PII: S0022-3115(98)00378-X

normal and grazing incidences. A threshold sputtering of 50 eV ion bombardment is considered. We adopted $1.0 \times 10^{18}$ ions/cm$^2$/s as a $D^+$ current density and the target temperature was set to be 300 K. This current density corresponds to the flux received by a divertor plate in a fusion reactor under steady-state operation. We assumed that the interstitial diffusion is dominant at this temperature and we neglect the vacancy diffusion and segregation. The respective acceptable activation energy of the B atom and the C atom are assumed to be 0.59 and 0.60 eV for interstitial diffusion [6].

In $B_4C$, the B atom is sputtered preferentially, because the surface binding energy of the B atom is lower than that of the C atom. The simulated $C_B^S/C_C^S$ ratios at the topmost layer is shown in Fig. 1 as a function of fluence at normal incidence, where 50, 80 and 200 eV are employed as the incident energies, and $C_B^S$ and $C_C^S$ are the surface concentrations of the B atom and the C atom, respectively. The inset in Fig. 1 shows the energy dependence of the total sputtering yields from the $B_4C$ material bombarded by an early irradiation whose fluence is denoted by $\Phi_0$ in the following discussion. The fluence $\Phi_0$ does not affect the surface concentration ratio. The total sputtering yields at 50, 80 and 200 eV are $4.8 \times 10^{-3}$, $1.1 \times 10^{-2}$ and $1.8 \times 10^{-2}$, respectively. The surface concentration ratio reaches a nearly constant steady-state value after a critical fluence denoted by $\Phi_{st}$. The critical fluences at 50, 80 and 200 eV are, approximately, $6.0 \times 10^{17}$, $1.6 \times 10^{17}$ and $1.0 \times 10^{17}$ ions/cm$^2$, which correspond to the removal of one surface layer due to sputtering.

The threshold energies of the B atom and the C atom for $D^+$ ion bombardment at normal incidence are 21.1 and 27.2 eV, respectively [7]. For low energies such as 50 eV $D^+$ the threshold effect enhances the preferential sputtering of B atoms. The relative sputtering yields, $Y_B/Y_C$, from the $B_4C$ material bombarded at $\Phi_0$ are 9.7, 5.7 and 4.7, respectively, for 50, 80 and 200 eV. This is why the steady-state surface concentration ratio of 50 eV is the lowest. Thus, the steady-state surface concentration ratio depends on the preferentiality of the sputtering.

Fig. 2 shows the surface concentration ratios $C_B^S/C_C^S$ at normal and grazing incidences for 50 and 200 eV, where the angle of incidence, $\theta$, is measured from the surface normal. The grazing angles are 65° and 75° for 50 and 200 eV, respectively. The normalized sputtering yield, $Y(\theta)/Y(0°)$, is shown in the inset of Fig. 2 as a function of the incident angle $\theta$. $Y(65°)/Y(0°)$ for 50 eV and $Y(75°)/Y(0°)$ for 200 eV are 2.9 and 8.1, respectively, and the relative sputtering yields $Y_B/Y_C$ for grazing incidence are 7.2 and 4.7, respectively, for 50 and 200 eV at $\Phi = \Phi_0$.

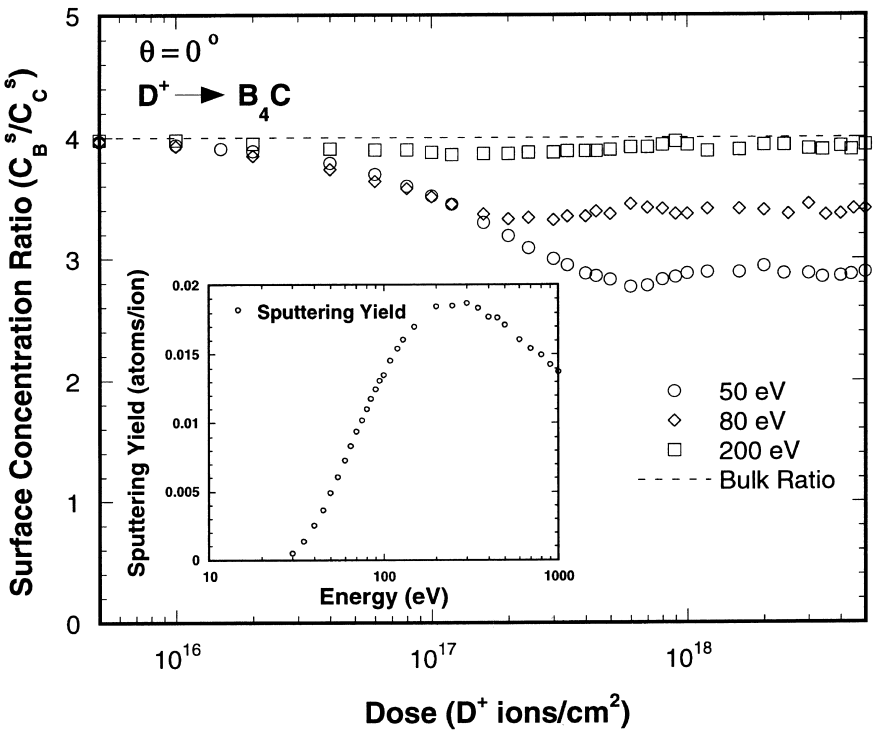


Fig. 1. Dose dependence of the $C_B^S/C_C^S$ ratio at the first layer during 50, 80 and 200 eV $D^+$ ion bombardments on $B_4C$ at normal incidence. The inset shows the energy dependence of the total sputtering yield of the $B_4C$ material bombarded by $\Phi_0$ with $D^+$ ion.

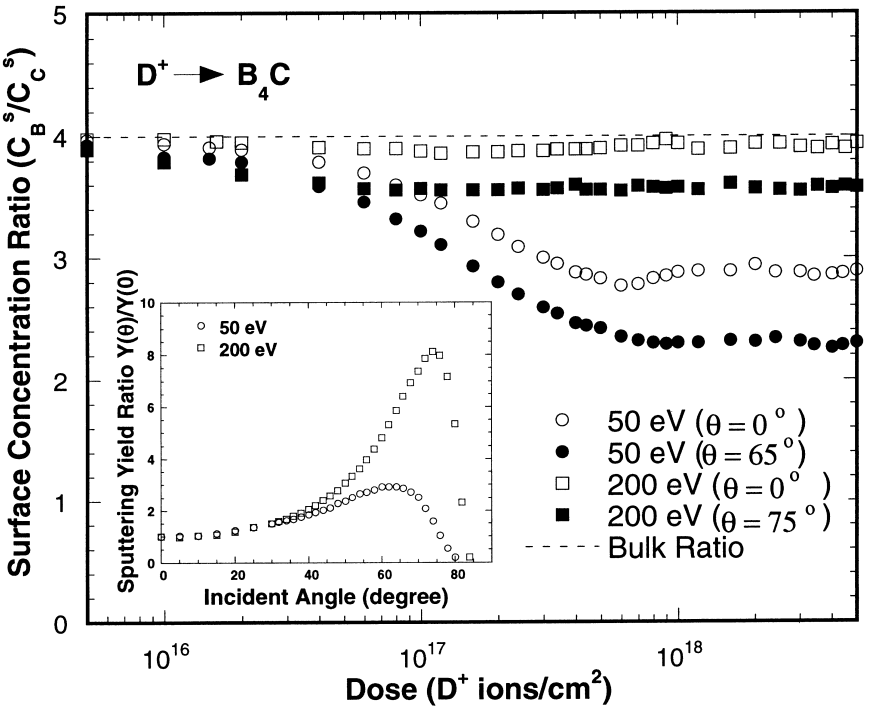


Fig. 2. Dose dependence of the surface concentration ratio $C_B^S/C_C^S$ during 50 and 200 eV $D^+$ ion bombardments on $B_4C$ at normal and grazing incidences, where the grazing angles are 65° for 50 eV and 75° for 200 eV. The inset shows the normalized sputtering yield, $Y(\Theta)/Y(0°)$, as a function of incident angle for 50 and 200 eV $D^+$ ion bombardment on the $B_4C$ material bombarded by $\Phi_0$ with $D^+$ ion.

When the ions are bombarded at grazing incidences, the energy deposition takes place only near the topmost layer and few interstitial atoms are produced in deeper layers. This means that the contribution of the diffusion seems to be very small. Therefore, the stationary surface concentrations are achieved only by the sputtering process and so the stationary values of $C_B^S/C_C^S$ at grazing incidences is lower than that of normal incidence, even if the preferentiality of sputtering at the grazing incidence is less than that of normal incidence. Inversely speaking, the stationary surface concentration at normal incidence is determined by the balance between the interstitial diffusion and the sputtering process.

As is known from Figs. 1 and 2, the surface B concentration at the steady state is less than that at $\Phi = \Phi_0$ for every case. This means that the total sputtering yields at $\Phi = \Phi_{st}$ are smaller than that at $\Phi = \Phi_0$; this is clearly shown in Table 1. Especially for a 50 eV ion bombardment, the sputtering yields are reduced by more than 20% at the steady state.

Fig. 3 shows the energy distributions of sputtered B and C atoms for 50 eV $D^+ \rightarrow B_4C$ under various bombarding conditions. In the case of light ion sputtering, almost all sputtered atoms are primary knocked-off recoil atoms due to reflected light ions, not due to the collision cascade. This is why the high energy tails of the

Table 1
The total sputtering yields at $\Phi = \Phi_{st}$ and $\Phi = \Phi_0$ for 50 and 200 eV ion bombardments on $B_4C$

| Incident energy (eV) | $\Theta$ (deg) | $\Phi_0$ | $\Phi_{st}$ |
|---|---|---|---|
| 50 | 0 | $4.8 \times 10^{-3}$ | $4.2 \times 10^{-3}$ |
| 200 | 0 | $1.8 \times 10^{-2}$ | $1.7 \times 10^{-2}$ |
| 50 | 65 | $1.5 \times 10^{-2}$ | $1.2 \times 10^{-2}$ |
| 200 | 75 | $1.5 \times 10^{-1}$ | $1.4 \times 10^{-1}$ |

energy spectra drop sharply compared with the Thompson formula [8].

The possible maximum energy of a sputtered atom at normal and grazing incidences will be roughly estimated by $(1 - \gamma)\gamma E$ and $\gamma E$, respectively, where $\gamma$ is the elastic energy transfer factor. The $\gamma E$'s of sputtered B and C atoms are 26.46 and 24.60 eV, respectively. The $(1 - \gamma)\gamma E$'s of sputtered B and C atoms are 12.46 and 12.50 eV, respectively. This is why the high energy edge of sputtered B atoms is larger than that of sputtered C atoms at grazing incidences and why the high energy edge at normal incidence is less than that at grazing incidence.

The difference of the energy spectra between $\Phi = \Phi_0$ and $\Phi = \Phi_{st}$ at grazing incidence is larger than that at normal incidence. This tendency reflects completely the

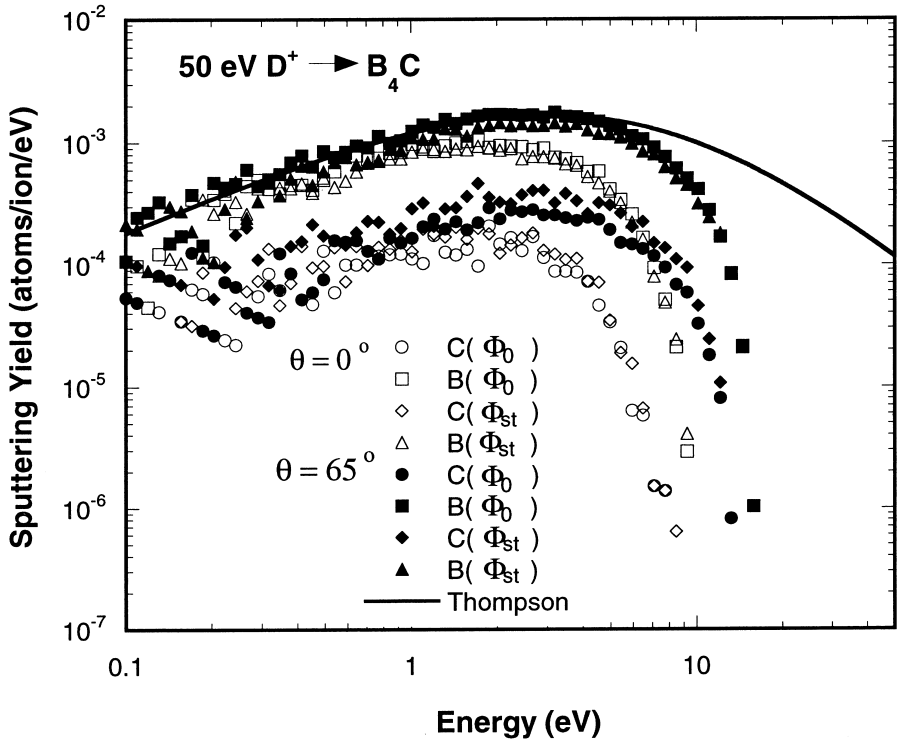


Fig. 3. Energy distributions of sputtered B and C atoms from $B_4C$ with 50 eV $D^+$ ion at normal and grazing incidences at various conditions. The angle of grazing incidence is 65°, and $\Phi_0$ and $\Phi_{st}$ refer to low fluence and the critical fluence, respectively. Symbols mean the ACAT-DIFFUSE data and the solid line means the Thompson formula.

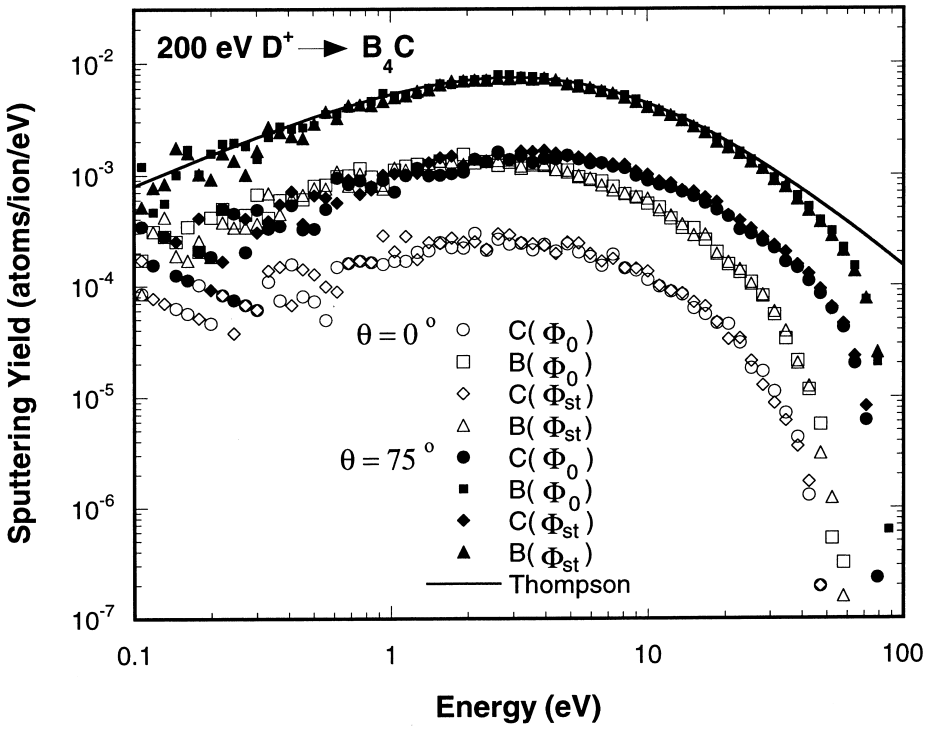


Fig. 4. The same as Fig. 3, but the incident energy is 200 eV and the angle of grazing incidence is 75°.

difference in the surface concentration ratios $C_B^S/C_C^S$ between $\Phi = \Phi_0$ and $\Phi = \Phi_{st}$ which is shown in Fig. 2.

Fig. 4 shows the energy distributions of sputtered B and C atoms for 200 eV $D^+ \rightarrow B_4C$ under various bombarding conditions. The high energy tails of the energy spectra for 200 eV also drop sharply. For 200 eV $D^+$, the $\gamma E$'s of sputtered B and C atoms are 105.9 and 98.4 eV, and the $(1 - \gamma)\gamma E$'s of sputtered B and C atoms are 49.8 and 50.0 eV, respectively. Therefore, there are similarities with the energy spectra at 50 eV.

It is well known that sputtered atoms that are ejected after sufficient collision processes will obey the Thompson formula and have a cosine angular distribution. It is interesting that the energy spectra of sputtered C atoms in Figs. 3 and 4 show slightly gentler slopes than those of sputtered B atoms in the higher energy region. Since the C atom density is one-quarter of B atoms in $B_4C$, an appreciable amount of C atoms will be sputtered by the two-step process, especially for the threshold sputtering such as in the 50 eV ion bombardment. Here, the two-step process means the following: First of all, the B atom with the major concentration is knocked off by the reflected $D^+$ ion and this knocked-off B atom hits the surface C atom with the minor concentration.

The angular distribution of sputtered atoms is sensitive to the concentration profile near the surface. In the case of the heavy ion sputtering, it shows the strong under-cosine distribution for low energy ion bombardment, and the cosine distribution for high energy ion bombardment. On the contrary, the light ion sputtering always shows the nearly cosine angular distribution, because the light ion sputtering is due to a single knock-on process. Figs. 5 and 6 show the angular distributions of sputtered B and C atoms at normal and grazing incidences for 50 and 200 eV $D^+$ ions, respectively. Though the angular distributions of C atoms at normal incidence for 50 eV have statistical errors near the surface normal, the angular distributions of both B and C atoms at normal incidence show slightly under-cosine distributions for 50 eV, and nearly cosine distributions for 200 eV. The difference in the angular distributions

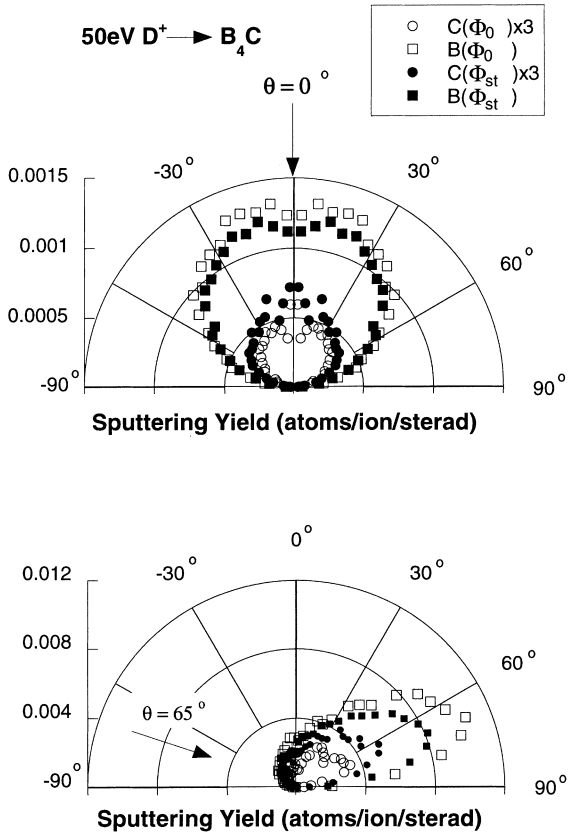


Fig. 5. Angular distributions of sputtered B and C atoms from $B_4C$ with 50 eV $D^+$ ion at normal and grazing incidences. The angle of grazing incidence is 65°, and $\Phi_0$ snd $\Phi_{st}$ are low fluence and the critical fluence, respectively. (sterad: steradian).

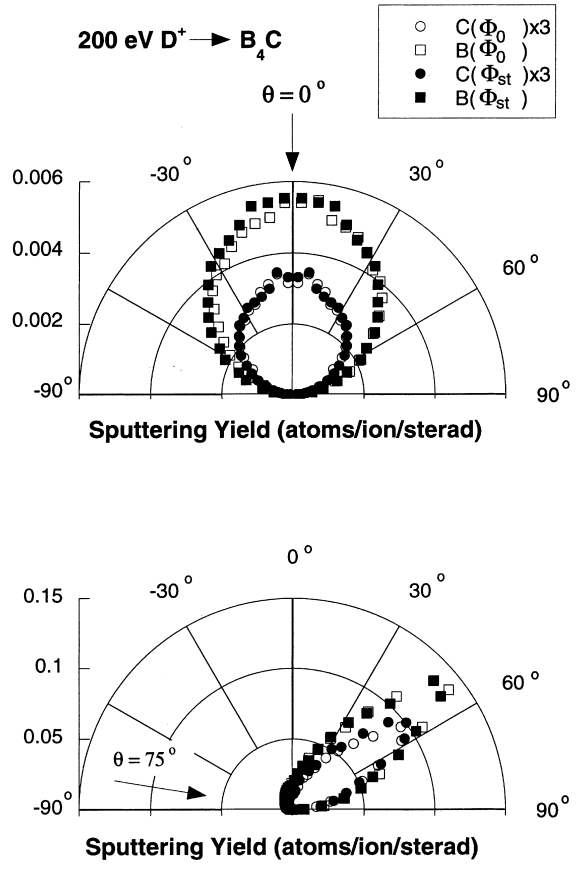


Fig. 6. The same as Fig. 5, but the incident energy is 200 eV and the angle of grazing incidence is 75°.

between $\Phi = \Phi_0$ and $\Phi = \Phi_{st}$ reflects completely the difference of the surface concentration ratios $C_B^S/C_C^S$ between $\Phi = \Phi_0$ and $\Phi = \Phi_{st}$.

The grazing light ion sputtering is mainly due to the direct knock-out process at the topmost surface layer [9]. The effect of two-step process is also observed in the angular distributions of sputtered C atoms of grazing incidence in Fig. 5. The two-step process makes the angular distribution of sputtered atoms broader.

## 4. Conclusions

Using the ACAT-DIFFUSE code, we simulated sputtering yields of $B_4C$ with near-threshold energy and relatively high energy at normal and grazing incidences. In the case of near-threshold sputtering, the preferential sputtering of B atoms is enhanced by the deference of a threshold energy between the C atom and the B atom, and so the steady-state surface B concentration is much less than the bulk concentration. As a result, the total sputtering yield at the steady-state is reduced by about 20% as compared with low-fluence sputtering. For high energy incidence the fluence effect is not observed appreciably.

The surface concentration at steady-state is determined by the competitive processes between diffusion and surface recession due to sputtering. At normal incidence there is an appreciable contribution from interstitial diffusion, but for grazing incidence because the energy deposition is limited to near the topmost surface and few interstitial atoms are produced in the deeper layer, the surface concentration is mainly determined by the preferential atom removal.

## References

[1] C. Garacia-Rosales, E. Gauthier, J. Roth, R. Schworer, W. Eckstein, J. Nucl. Mater 189 (1992) 1.
[2] Y. Ohtuka, M. Isobe, K. Nakano, Y. Ueda, S. Goto, M. Nishikawa, J. Nucl. Mater 222 (1995) 886.
[3] M. Isobe, Y. Ohtuka, H. Shinonaga, Y. Ueda, B. Kyoh, M. Nishikawa, Fusion Eng. Des. 28 (1995) 170.
[4] Y. Yamamura, T. Kenmotsu, Rad. Eff. Defects. Solids 142 (1997) 385.
[5] Y. Yamamura, Nucl. Instr. and Meth. B 28 (1987) 17.
[6] A. Von Oertzen, H.H. Rotermund, S. Nettesheim, Surf. Sci. 311 (1994) 322.
[7] Y. Yamamura, J. Bohdansky, Vacuum 35 (1985) 561.
[8] G. Falcone, P. Sigmund, Appl. Phys. 25 (1981) 307.
[9] Y. Yamamura, N. Itoh, Sputtering yield, in: T. Itoh (Ed.), Ion Beam Assisted Film Growth, ch. 4, Elsevier, Amsterdam, 1989.